Turkish J. Eng. Env. Sci.
35 (2011) , 187 – 198.

doi:10.3906/muh-1101-15

Free convection flow past an impulsively started infinite vertical plate with Newtonian heating in the presence of thermal radiation and mass diffusion

Marneni NARAHARI*, **M. Yunus NAYAN**
Fundamental and Applied Sciences, Universiti Teknologi PETRONAS,
31750 Tronoh-MALAYSIA
e-mails: marneni@petronas.com.my, yunusna@petronas.com.my

Received: 18.01.2011

Abstract

An analytical study of free convection flow near an impulsively started infinite vertical plate with Newtonian heating in the presence of thermal radiation and constant mass diffusion was performed. The mathematical model reduced to a system of coupled linear partial differential equations for the velocity, the temperature, and the concentration; the closed-form exact solutions were obtained by the Laplace transform method. Representative velocity and temperature profiles were graphed and the numerical values of the skin friction and the Nusselt number were calculated. The effects of different system parameters, such as the radiation parameter, buoyancy ratio, Grashof number, Prandtl number, Schmidt number and time on the velocity, temperature, skin friction, and Nusselt number, were examined in detail. It was observed that the velocity increased for aiding flows, whereas it decreased for opposing flows. The velocity decreased with increasing Schmidt number and radiation parameter. The skin friction decreased in the presence of aiding flows whereas it increased in the presence of opposing flows. Furthermore, the skin friction increased with increasing Schmidt number and radiation parameter.

Key Words: Unsteady free convection flow, Newtonian heating, thermal radiation, heat transfer, mass transfer, impulsively started vertical plate

1. Introduction

The analysis of natural convection heat and mass transfer near a moving vertical plate has received much attention in recent times due to its wide application in engineering and technological processes. There are applications of interest in which combined heat and mass transfer by natural convection occurs between a moving material and the ambient medium, such as the design and operation of chemical processing equipment, design of heat exchangers, transpiration cooling of a surface, chemical vapor deposition of solid layers, nuclear reactors, and many manufacturing processes like hot rolling, hot extrusion, wire drawing, continuous casting, and fiber drawing. Gebhart and Pera (1971) studied the effects of mass transfer on a steady free convection flow

*Corresponding author

past a semiinfinite vertical plate by the similarity method, and it was assumed that the concentration level of the diffusing species in the fluid medium was very low. This assumption enabled them to neglect the diffusion-thermo and the thermo-diffusion effects, as well as the interfacial velocity at the wall due to species diffusion. Following this assumption, Soundalgekar (1979) studied the effects of mass transfer on the free convection flow past an impulsively started infinite vertical plate and presented an exact solution by the Laplace transform method. Soundalgekar and his co-researchers (1984, 1992, 1994, 1996, 2000, 2001) investigated the effects of simultaneous heat and mass transfer on free convection flow past an infinite vertical plate under different physical situations.

When the temperature of the surrounding fluid is rather high, radiation effects play an important role, and this situation exists in space technology applications such as cosmic flight aerodynamics, rocket propulsion systems, plasma physics, and space craft reentry aerothermodynamics. In these cases, it is necessary to consider the radiation effects in free convection flows. Cess (1966) investigated the interaction of radiation with laminar free convection heat transfer from a vertical plate for an absorbing, emitting fluid in the optically thick region, using the singular perturbation technique. Arpaci (1968) considered a similar problem in both the optically thin and optically thick regions and used the approximate integral technique and first-order profiles to solve the energy equation. Das et al. (1996) analyzed the radiation effects on flow past an impulsively started infinite isothermal vertical plate, and the governing equations were solved by the Laplace transform technique. Hossain et al. (1999) determined the effect of radiation on the natural convection flow of an optically thick, viscous, incompressible flow past a heated vertical porous plate with a uniform surface temperature and a uniform rate of suction, where the radiation was included by assuming the Rosseland diffusion approximation. Raptis and Perdikis (1999) studied the effects of thermal radiation and free convective flow past a uniformly accelerated vertical plate. Chamkha et al. (2001) studied radiation effects on the free convection flow past a semiinfinite vertical plate in the presence of a low-level chemical species concentration. Loganathan and Ganesan (2006) considered the effect of radiation on the free convection flow past an impulsively started vertical plate in the presence of mass transfer. A 2-dimensional analysis of heat and mass transfer inside a rectangular moist object under the drying process was presented by Kaya et al. (2006) using an implicit finite difference method. Prasad et al. (2007) examined the radiation and mass transfer effects on the unsteady 2-dimensional free convection flow of a viscous incompressible fluid past an impulsively started infinite vertical plate. Recently, Narahari and Dutta (2009) presented a theoretical solution to the free convection flow of a viscous incompressible fluid past an infinite vertical moving plate subject to a ramped surface temperature with simultaneous mass transfer using the Laplace transform technique.

In Newtonian heating, the rate of heat transfer from the bounding surface with a finite heat capacity is proportional to the local surface temperature, and it is usually called conjugate convective flow. Merkin (1994) was the first to consider the free convection boundary layer over a vertical flat plate immersed in a viscous fluid. Lesnic et al. (1999, 2000) considered free convection boundary layer flow along vertical and horizontal surfaces in a porous medium generated by Newtonian heating. The steady free convection boundary layer along a semiinfinite plate, slightly inclined to the horizontal and embedded in a porous medium with the flow generated by Newtonian heating, was investigated by Lesnic et al. (2004). Chaudhary and Jain (2007) presented an exact solution for the unsteady free convection boundary layer flow of an incompressible fluid past an infinite vertical plate with the flow generated by Newtonian heating and the impulsive motion of the plate. An exact solution of the unsteady free convection flow of a viscous incompressible, optically thin, radiating fluid past an impulsively started vertical porous plate with Newtonian heating was investigated by Mebine and

Adigio (2009). A numerical solution to the steady mixed convection boundary layer flow over a horizontal circular cylinder with Newtonian heating was presented by Salleh et al. (2010). The steady laminar boundary layer flow and heat transfer over a stretching sheet with Newtonian heating was also considered by Salleh et al. (2010). A mathematical model for the forced convection boundary layer flow over a circular cylinder with Newtonian heating in a uniform stream was presented by Salleh et al. (2011). Recently, the influence of thermal radiation on unsteady free convection flow past a moving vertical plate with Newtonian heating was investigated by Narahari and Ishak (2011). However, the effects of mass transfer on the flow of a viscous incompressible, radiating fluid past an impulsively started infinite vertical plate with Newtonian heating have not been studied in the literature. This indeed was the motivation to study such effects on the flow past an impulsively started infinite vertical plate. Closed-form solutions were obtained by the Laplace transform method and the solutions can be used as test cases for numerical solutions of higher order models.

2. Mathematical analysis

Consider the flow of a viscous incompressible fluid past an infinite vertical plate with Newtonian heating in the presence of thermal radiation and mass diffusion. The x'-axis is along the plate in the vertically upward direction and the y'-axis is taken as normal to the plate. Initially, the plate and the adjacent fluid are at the same temperature, T'_∞, and concentration, C'_∞, in a stationary condition. At time $t' > 0$, the plate is given an impulsive motion in the vertical direction against the gravitational field, such that it attains uniform velocity U_0 and the concentration level near the plate is raised to $C'_w(\neq C'_\infty)$, and it is assumed that the heat transfer from the surface is proportional to the local surface temperature, T'. As the plate is infinite in the x'-direction, all physical variables are independent of x' and are functions of y' and t' only. Under the usual Boussinesq approximation, after neglecting the inertia terms, viscous dissipation heat, and Soret and Dufour effects, the flow can be shown to be governed by the following system of equations:

$$\frac{\partial u'}{\partial t'} = \nu \frac{\partial^2 u'}{\partial y'^2} + g\beta(T' - T'_\infty) + g\beta^*(C' - C'_\infty), \tag{1}$$

$$\rho C_p \frac{\partial T'}{\partial t'} = k\frac{\partial^2 T'}{\partial y'^2} - \frac{\partial q_r}{\partial y'}, \tag{2}$$

$$\frac{\partial C'}{\partial t'} = D\frac{\partial^2 C'}{\partial y'^2}, \tag{3}$$

with the initial and boundary conditions:

$$\left.\begin{array}{ll} t' \le 0 : u' = 0,\ T' = T'_\infty,\ C' = C'_\infty & \text{for } \ y' \ge 0, \\ t' > 0 : \begin{cases} u' = U_0,\ \frac{\partial T'}{\partial y'} = -\frac{h}{k}T',\ C' = C'_w & \text{at } \ y' = 0, \\ u' \to 0,\ T' \to T'_\infty,\ C' \to C'_\infty & \text{as } \ y' \to \infty. \end{cases} \end{array}\right\}. \tag{4}$$

The radiative heat flux term is simplified by making use of the Rosseland approximation (Siegel and Howell, 2002) as:

$$q_r = -\frac{4\sigma}{3K_R}\frac{\partial T'^4}{\partial y'}. \tag{5}$$

It should be noted that by using the Rosseland approximation, we limit our analysis to optically thick fluids. If temperature differences within the flow are sufficiently small, such that T'^4 may be expressed as a linear function of the temperature, then the Taylor series for T'^4 about T'_∞, after neglecting higher order terms, is given by:

$$T'^4 \cong 4T'^3_\infty T' - 3T'^4_\infty. \tag{6}$$

In view of Eqs. (5) and (6), Eq. (2) reduces to:

$$\rho C_p \frac{\partial T'}{\partial t'} = k\frac{\partial^2 T'}{\partial y'^2} + \frac{16\sigma T'^3_\infty}{3K_R}\frac{\partial^2 T'}{\partial y'^2}. \tag{7}$$

All of the physical quantities are defined in the nomenclature. Upon introducing the following nondimensional equalities:

$$\left.\begin{array}{l} y = \frac{y'U_0}{\nu},\ t = \frac{t'U_0^2}{\nu},\ u = \frac{u'}{U_0\,Gr},\ \theta = \frac{T'-T'_\infty}{T'_\infty},\ \mathrm{Pr} = \frac{\mu C_p}{k},\ Gr = \frac{\nu g\beta T'_\infty}{U_0^3}, \\ R = \frac{k\,K_R}{4\sigma T'^3_\infty},\ C = \frac{C'-C'_\infty}{C'_w-C'_\infty},\ Gm = \frac{\nu g\beta^*(C'_w-C'_\infty)}{U_0^3},\ \mathrm{Sc} = \frac{\nu}{D},\ N = \frac{Gm}{Gr}. \end{array}\right\}, \tag{8}$$

Eqs. (1), (7), and (3) are reduced to the following nondimensional forms:

$$\frac{\partial u}{\partial t} = \frac{\partial^2 u}{\partial y^2} + \theta + NC, \tag{9}$$

$$3R\,\mathrm{Pr}\,\frac{\partial \theta}{\partial t} = (3R+4)\frac{\partial^2 \theta}{\partial y^2}, \tag{10}$$

$$Sc\frac{\partial C}{\partial t} = \frac{\partial^2 C}{\partial y^2}. \tag{11}$$

The corresponding initial and boundary conditions are:

$$\left.\begin{array}{lll} t \le 0: & u = 0,\ \theta = 0,\ C = 0 & \text{for}\quad y \ge 0, \\ t > 0: & \left\{\begin{array}{l} u = \frac{1}{Gr},\ \frac{\partial\theta}{\partial y} = -(1+\theta),\ C = 1 \\ u \to 0,\ \theta \to 0,\ C \to 0 \end{array}\right. & \begin{array}{l}\text{at}\quad y = 0, \\ \text{as}\quad y \to \infty. \end{array} \end{array}\right\}. \tag{12}$$

Coupled linear partial differential Eqs. (9-11) are solved subject to the initial and boundary conditions of Eq. (12) by the usual Laplace transform method (Abramowitz and Stegun, 1972), and the solutions are given as follows:

$$C(y,t) = f_1(y\sqrt{\mathrm{Sc}}, t), \tag{13}$$

$$\theta(y,t) = f_4(y\sqrt{A}, t) - f_1(y\sqrt{A}, t). \tag{14}$$

Case 1: Sc $\neq 1$

$$\begin{array}{rcl} u(y,t) & = & \frac{1}{Gr}f_1(y,t) + \frac{A}{(A-1)}\left[f_1(y\sqrt{A},t) - f_1(y,t) - f_4(y\sqrt{A},t) + f_4(y,t)\right] \\ & & +\frac{\sqrt{A}}{(A-1)}\left[f_2(y\sqrt{A},t) - f_2(y,t)\right] + \frac{1}{(A-1)}\left[f_3(y\sqrt{A},t) - f_3(y,t)\right] \\ & & +\frac{N}{(\mathrm{Sc}-1)}\left[f_3(y,t) - f_3(y\sqrt{\mathrm{Sc}},t)\right] \end{array}, \tag{15a}$$

Case 2: $\mathrm{Sc}=1$

$$\begin{aligned} u(y,t) \quad = \quad & \tfrac{1}{Gr} f_1(y,t) + \tfrac{A}{(A-1)}\left[f_1(y\sqrt{A},t) - f_1(y,t) - f_4(y\sqrt{A},t) + f_4(y,t)\right] \\ & + \tfrac{\sqrt{A}}{(A-1)}\left[f_2(y\sqrt{A},t) - f_2(y,t)\right] + \tfrac{1}{(A-1)}\left[f_3(y\sqrt{A},t) - f_3(y,t)\right] \quad , \\ & + \tfrac{Ny}{2} f_2(y,t) \end{aligned} \tag{15b}$$

where $A=\frac{3R\,\mathrm{Pr}}{3R+4}$,

$$f_1(z,t)=\mathrm{erfc}\left(\frac{z}{2\sqrt{t}}\right),$$

$$f_2(z,t)=2\sqrt{t/\pi}\exp\left(-\frac{z^2}{4t}\right)-z\,\mathrm{erfc}\left(\frac{z}{2\sqrt{t}}\right),$$

$$f_3(z,t)=\left(\frac{z^2}{2}+t\right)\mathrm{erfc}\left(\frac{z}{2\sqrt{t}}\right)-z\sqrt{t/\pi}\exp\left(-\frac{z^2}{4t}\right),$$

$$f_4(z,t)=\exp\left(\frac{t}{A}-\frac{z}{\sqrt{A}}\right)\mathrm{erfc}\left(\frac{z}{2\sqrt{t}}-\sqrt{\frac{t}{A}}\right),$$

z is a dummy variable, and f_1, f_2, f_3, f_4 are dummy functions. Moreover, the concentration variable given by Eq. (13) is well known (Soundalgekar, 1979).

From the velocity field, it is interesting to study the effects of the system parameters on the skin friction. It is given by:

$$\tau=\frac{\tau'}{\rho\,GrU_0^2}=-\left.\frac{\partial u}{\partial y}\right|_{y=0}. \tag{16}$$

From Eqs. (15) and (16), we have:

$$\tau=\frac{1}{Gr\sqrt{\pi t}}+\frac{\sqrt{A}}{\sqrt{A}+1}\left[1+2\sqrt{\frac{t}{A\pi}}-\exp\left(\frac{t}{A}\right)\left(1+\mathrm{erf}\left(\sqrt{\frac{t}{A}}\right)\right)\right]-\frac{2N\sqrt{t}}{\sqrt{\pi}(\sqrt{\mathrm{Sc}}+1)}. \tag{17}$$

From the temperature field, the rate of heat transfer in the form of the Nusselt number can be expressed as:

$$Nu=-\frac{\nu}{U_0(T'-T'_\infty)}\left.\frac{\partial T'}{\partial y'}\right|_{y=0}=\frac{1}{\theta(0,t)}+1=\frac{1}{\exp(t/A)(1+\mathrm{erf}(\sqrt{t/A}))-1}+1. \tag{18}$$

2.1. Solution in the absence of thermal radiation

In the absence of thermal radiation, i.e. in the pure convection case that numerically corresponds to $R\to\infty$, it can be observed that $A=\mathrm{Pr}$, and the solution for the temperature variable given by Eq. (14) is valid for all values of Pr, but the solution for the velocity variable given by Eq. (15) is valid for all values of Pr except for $\mathrm{Pr}=1$. Therefore, the solution for the velocity variable in the absence of thermal radiation when $\mathrm{Pr}=1$ has to be rederived, and it can be shown that:

Case 3: $\mathrm{Pr}=1$, $\mathrm{Sc}\neq 1$

$$\begin{aligned} u(y,t) = & \tfrac{1}{Gr} f_1(y,t) + \tfrac{y}{2}\left[f_5(y,t) - f_1(y,t) - f_2(y,t)\right] \\ & + \tfrac{N}{(\mathrm{Sc}-1)}\left[f_3(y,t) - f_3(y\sqrt{\mathrm{Sc}},t)\right] \quad , \end{aligned} \tag{19}$$

Case 4: $\Pr = 1, \mathrm{Sc} = 1$

$$u(y,t) = \frac{1}{Gr} f_1(y,t) + \frac{y}{2}\left[f_5(y,t) - f_1(y,t) - f_2(y,t)\right] + \frac{N\,y}{2} f_2(y,t) \quad , \tag{20}$$

where $f_5(z,t) = \exp(t-z)\mathrm{erfc}\left(\frac{z}{2\sqrt{t}} - \sqrt{t}\right)$ is a dummy function.

3. Results and discussion

In order to determine the effect of different parameters, such as R, N, Gr, Pr, Sc, and t on the free convection flow, the numerical values of the temperature field, velocity field, skin friction, and Nusselt number were computed and are shown in the Figures and Tables. The temperature profiles are plotted in Figure 1 for different values of t and Pr when $R = 10$. It can be observed that the thermal boundary layer thickness decreases in terms of y at increasing distances from the leading edge. Furthermore, the thermal boundary layer thickness decreases with an increase in the Prandtl number. This is consistent with the fact that smaller Prandtl numbers are equivalent to increases in thermal conductivities, and therefore heat is able to diffuse away from the heated surface more rapidly than for higher values of the Prandtl number. When $t = 0.2$ and $R = 10$, the thermal boundary layer decreases by 87.36% and 96.12% when Pr increases from 0.71 (air) to 7 (water) and 50 (oils), respectively, at the plate ($y = 0$). It was also observed that the temperature increased with increasing time. When radiation effects are present in a fluid with $\Pr = 0.71$ and $R = 10$, the thermal boundary layer increases by 96.66% and 223.36% when t increases from 0.2 to 0.4 and 0.6, respectively, at the plate.

The temperature profiles are plotted in Figure 2 for different values of R and Pr when $t = 0.2$. It can be seen that an increase in the radiation parameter decreases the temperature. Therefore, increases in the value of R lead to a decrease in the thermal boundary layer thicknesses. When radiation effects are present in a fluid, the thermal boundary layer is always found to thicken. The reason for this is that radiation provides an additional means to diffuse energy. From the calculated values of the temperature at the plate when $t = 0.2$, and $\Pr = 0.71$ and 7.0, for $R = 0.5$, 1.0, and 10, the thermal boundary layer is found to thicken by 299.33%, 125.95%, and 11.2%, and by 124.84%, 67.23%, and 7.61%, respectively, of the pure convection case (which numerically corresponds to $R \to \infty$).

The buoyancy ratio parameter N represents the ratio of the mass and the thermal buoyancy forces, and there are 3 possible cases: 1) $N = 0$ (there is no mass transfer and the buoyancy force is due to thermal diffusion only), 2) $N > 0$ (the mass buoyancy force acts in the same direction as the thermal buoyancy force), or 3) $N < 0$ (the mass buoyancy force acts in the opposite direction of thermal buoyancy force). The velocity profiles are plotted in Figure 3 for different values of t and Gr when $\Pr = 0.71$, $R = 10$, and $\mathrm{Sc} = 0.6$ for the cases of both aiding ($N > 0$) and opposing ($N < 0$) flows. It can be seen that the velocity increases with increased time for both aiding and opposing flows. Moreover, the velocity distribution is monotonic at lower times, but at a higher time it passes through a maximum in the vicinity of the plate when the buoyancy effect partly suppresses the inertial effects of the plate velocity. Thus, when radiation effects are present in a fluid with $\Pr = 0.71$, $\mathrm{Sc} = 0.6$, $N = 0.2$ (aiding flow), and $R = 10$, the momentum boundary layer thickness increases by 36.06% and 75.52% when t increases from 0.2 to 0.4 and 0.6, respectively, at $y = 0.3$; and for $\Pr = 0.71$, $\mathrm{Sc} = 0.6, N = -0.2$ (opposing flow), and $R = 10$, the momentum boundary layer thickness increases by 34.22% and 72.82% when t increases from 0.2 to 0.4 and 0.6, respectively, at $y = 0.3$. It was also seen that increasing values of Gr led to a decrease in the velocity. When $\Pr = 0.71$, $\mathrm{Sc} = 0.6$, $R = 10$, and $t = 0.2$, the fluid velocity decreases by 44.25% for an aiding flow with $N = 0.2$ and by 46.72% for an opposing flow with $N = -0.2$ when Gr increases from 2 to 4 at $y = 0.3$.

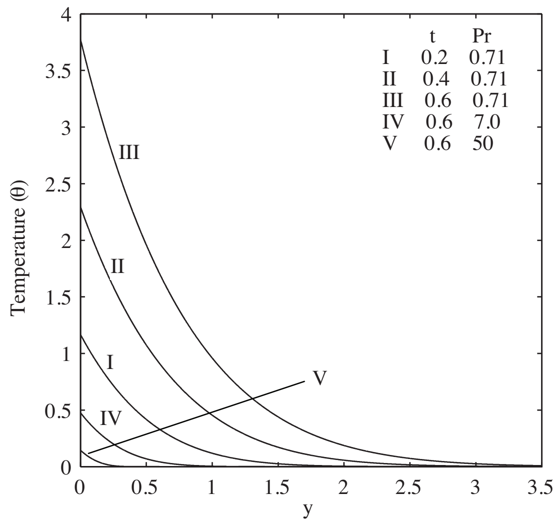

Figure 1. Temperature profiles for different t and Pr when $R = 10$.

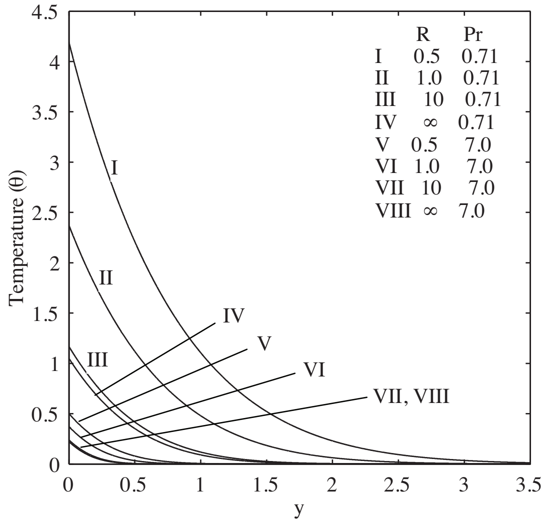

Figure 2. Temperature profiles for different R and Pr when $t = 0.2$.

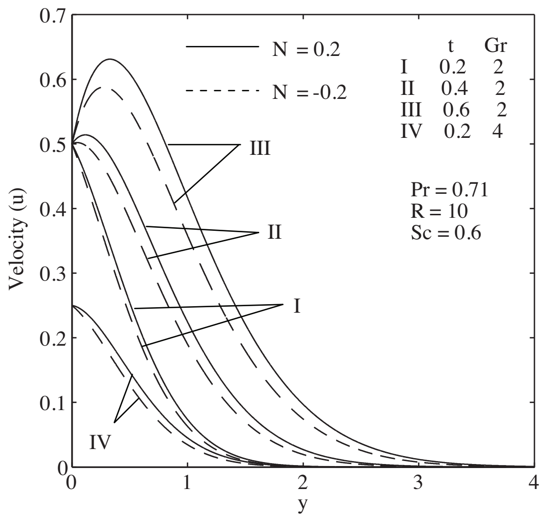

Figure 3. Velocity profiles for different t and Gr.

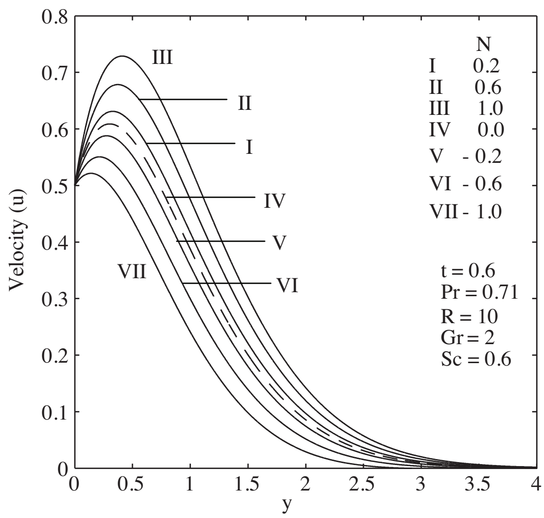

Figure 4. Velocity profiles for different N.

The velocity profiles are plotted in Figure 4 for different values of N when $t = 0.6$, $\Pr = 0.71$, $Gr = 2$, $\mathrm{Sc} = 0.6$, and $R = 10$. It can be clearly seen that the velocity increases with increasing values of N for aiding flows. This is the reason for the large buoyancy force caused by the concentration difference. In the case of opposing flows, the velocity decreases with the increase in the opposing buoyancy force. Thus, when $t = 0.6$, $\Pr = 0.71$, $Gr = 2$, $\mathrm{Sc} = 0.6$, and $R = 10$, the momentum boundary layer thickness increases by 3.53%, 10.56%, and 17.61% when N increases from 0 to 0.2, 0.4, and 0.6, whereas the momentum boundary layer decreases by 3.52%, 10.55%, and 17.59% when N decreases from 0 to –0.2, –0.4, and –0.6, respectively, at $y = 0.3$.

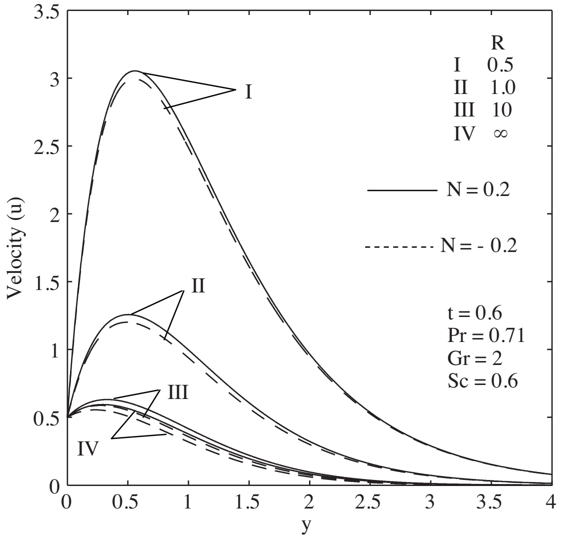

Figure 5. Velocity profiles for different R and N.

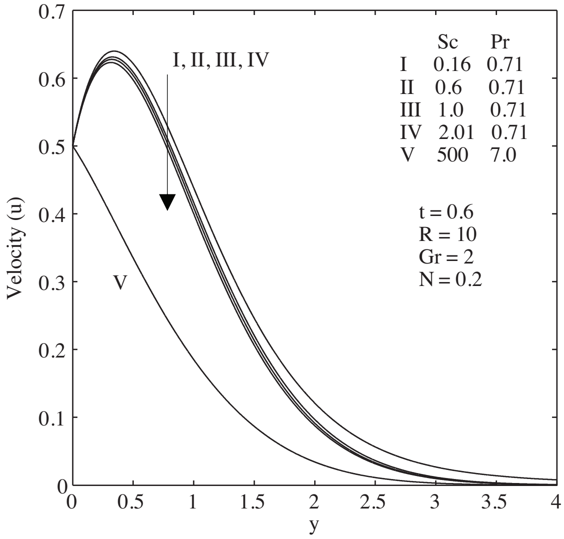

Figure 6. Velocity profiles for different Sc and Pr.

The velocity distributions are plotted in Figure 5 for different values of R when $t = 0.6$, $\mathrm{Pr} = 0.71$, $Gr = 2$, and $\mathrm{Sc} = 0.6$ for both aiding and opposing flows. It can be observed that an increase in the radiation parameter decreases the velocity. This result may be explained by the fact that an increase in the radiation parameter $R\,(= kK_R/4\sigma T_\infty'^3)$ for fixed k and T_∞' values means an increase in the Rosseland mean attenuation coefficient K_R. Therefore, the rate of radiative heat transferred to the fluid decreases, and consequently the fluid velocity decreases along with the temperature. Thus, increases in the value of R lead to a decrease in the momentum boundary layer thickness. From the calculated values of the velocity when $t = 0.6$, $\mathrm{Pr} = 0.71$, $Gr = 2$, and $\mathrm{Sc} = 0.6$, the velocity increases by 6.08%, 96.23%, and 349.50% for an aiding flow with $N = 0.2$, and by 6.53%, 103.70%, and 376.62% for an opposing flow with $N = -0.2$ when the radiation parameter R decreases from ∞ to 10, 1.0, and 0.5, respectively, at $y = 0.3$. The velocity profiles for different values of Sc and Pr are plotted in Figure 6 when $t = 0.6$, $Gr = 2$, $R = 10$, and $N = 0.2$. It can be observed that there is a decrease in the velocity of air and water due to an increase in the value of the Schmidt number. An increasing Schmidt number implies that viscous forces dominate over the diffusional effects.

The variation of the skin friction at the plate is shown in Table 1 for various values of the governing parameters. It was observed that the skin friction decreased as the time progressed for both aiding and opposing flows. However, the skin friction was greater for an opposing flow when compared with an aiding flow at a given time. The skin friction increased with increasing values of Pr, whereas the friction decreased with the increase in the value of *Gr*. An increase in the radiation parameter led to an increase in the skin friction in the presence of an aiding flow. Thus, when $t = 0.2$, $\mathrm{Pr} = 0.71$, $Gr = 2$, $\mathrm{Sc} = 0.6$, and $N = 0.2$, the skin friction is found to decrease by 7.62%, 84.96%, and 197.32% when the radiation parameter R decreases from ∞ to 10, 1.0, and 0.5, respectively. The skin friction decreases for aiding flows, whereas it increases for opposing flows. From the calculated values of the skin friction when $t = 0.2$, $\mathrm{Pr} = 0.71$, $Gr = 2$, $\mathrm{Sc} = 0.6$, and $R = 10$, the skin-friction decreases by 14.35% and 43.06% for aiding flows when N increases from 0 to 0.2 and 0.6, whereas the skin friction increases by 14.35% and 43.06% for opposing flows when N decreases from 0 to –0.2 and –0.6, respectively. It was also observed that the skin friction increased with an increase in the value of Sc for an aiding flow at a given time. This result may be explained by the fact that an increasing value of Sc implies a reduced mass buoyancy effect, and hence there is more friction at the moving plate.

The variation of the Nusselt number at the plate is shown in Table 2 for different values of t, Pr, and R. It can be observed that the Nusselt number increases with increasing values of Pr. This may be explained by the fact that frictional forces become dominant with increasing values of Pr and hence yield greater heat transfer

Table 1. Skin friction variation.

t	Pr	Gr	R	N	Sc	τ
0.01	0.71	2	10	0.2	0.6	2.800447
0.1	0.71	2	10	0.2	0.6	0.752771
0.2	0.71	2	10	0.2	0.6	0.339393
0.3	0.71	2	10	0.2	0.6	0.039541
0.4	0.71	2	10	0.2	0.6	–0.251251
0.2	0.71	2	10	0	–	0.396265
0.01	0.71	2	10	–0.2	0.6	2.825881
0.1	0.71	2	10	–0.2	0.6	0.833200
0.2	0.71	2	10	–0.2	0.6	0.453137
0.3	0.71	2	10	–0.2	0.6	0.178849
0.4	0.71	2	10	–0.2	0.6	–0.090392
0.2	0.71	4	10	0.2	0.6	0.024001
0.2	0.71	2	0.5	0.2	0.6	–0.357562
0.2	0.71	2	1.0	0.2	0.6	0.055275
0.2	0.71	2	∞	0.2	0.6	0.367400
0.2	0.71	2	10	0.2	0.16	0.324176
0.2	0.71	2	10	0.2	1.0	0.345802
0.2	0.71	2	10	0.2	2.01	0.354521
0.2	7.0	2	10	0.2	500	0.599828
0.2	0.71	2	10	0.6	0.6	0.225648
0.2	0.71	2	10	–0.6	0.6	0.566882

Table 2. Nusselt number variation.

t	Pr	R	Nu
0.01	0.71	10	7.242990
0.1	0.71	10	2.481318
0.2	0.71	10	1.855892
0.3	0.71	10	1.588433
0.4	0.71	10	1.435191
0.2	7.0	10	5.159733
0.4	7.0	10	3.726401
0.2	50	10	13.384291
0.4	50	10	9.532214
0.2	0.71	0.5	1.238377
0.2	0.71	1.0	1.421293
0.2	0.71	∞	1.951950
0.2	7.0	0.5	2.990932
0.2	7.0	1.0	3.676759
0.2	7.0	∞	5.476492
0.2	50	0.5	7.545690
0.2	50	1.0	9.398446
0.2	50	∞	14.233887

rates. It was also observed that the Nusselt number decreased as the time proceeded, whereas it increased with an increase in the radiation parameter for all values of Pr at an early time. From the calculated values, when $t = 0.2$ the Nusselt number decreases by 4.92%, 27.19%, and 36.56% for $\mathrm{Pr} = 0.71$, by 5.78%, 32.86%, and 45.39% for $\mathrm{Pr} = 7.0$, and by 5.97%, 33.97%, and 46.99% for $\mathrm{Pr} = 50$ when the radiation parameter R decreases from ∞ to 10, 1.0, and 0.5, respectively. It is interesting to note that the percentage decrease in the Nusselt number from the pure convection case ($R \to \infty$) increases with an increasing Pr value for any fixed value of the radiation parameter.

4. Conclusions

The problem of unsteady free convection heat and mass transfer along an impulsively started infinite vertical plate with Newtonian heating in the presence of thermal radiation was analyzed. The governing system of linear partial differential equations was solved analytically with the help of the Laplace transform method without any restrictions. The effects of the system parameters on the velocity and temperature fields, the skin friction, and the Nusselt number were studied in detail. The results indicate that the radiation parameter (R), buoyancy ratio (N), and Schmidt number (Sc) had significant influences on the velocity and temperature fields, the skin friction, and the Nusselt number. It was observed that an increase in the radiation parameter served to thin the thermal and momentum boundary layers. The velocity of the fluid was enhanced, whereas the skin friction diminished as the buoyancy ratio increased. Increasing Schmidt numbers led to a decrease in the velocity and an increase in the skin friction when radiation effects were present. The Nusselt number decreased as the radiation parameter decreased. It is hoped that these results will have immediate relevance in space technology, transient energy systems, and industrial thermo-fluid dynamics.

Nomenclature

C'	species concentration (kg m^{-3})
C	dimensionless concentration
C'_∞	species concentration away from the plate
C_p	specific heat of the fluid at constant pressure (J kg^{-1} K^{-1})
D	mass diffusivity (m^2 s^{-1})
g	gravitational acceleration (m s^{-2})
h	heat transfer coefficient (W m^{-2} K^{-1})
k	thermal conductivity (W m^{-1} K^{-1})
K_R	Rosseland mean attenuation coefficient (m^{-1})
N	buoyancy ratio parameter
Nu	Nusselt number
Pr	Prandtl number
q_r	radiative flux (W m^{-2})
R	radiation parameter
Sc	Schmidt number
t'	time (s)
t	dimensionless time
T'	temperature of the fluid near the plate (K)
T'_∞	temperature of the fluid away from the plate
u'	velocity in the x'-direction (m s^{-1})
u	dimensionless velocity
U_0	velocity of the plate
y	dimensionless coordinate axis normal to the plate

Greek symbols

β	volumetric coefficient of thermal expansion (K^{-1})
β^*	volumetric coefficient of concentration expansion (m^3 kg^{-1})
θ	dimensionless temperature
μ	coefficient of viscosity (kg m^{-1} s^{-1})
ν	kinematic viscosity (m^2 s^{-1})
ρ	fluid density (kg m^{-3})
σ	Stefan-Boltzmann constant (W m^{-2} K^{-4})
τ'	shear stress (kg m^{-1} s^{-2})
τ	dimensionless skin friction

References

Abramowitz, M. and Stegun, I.A., Handbook of Mathematical Functions, Dover Publications, New York, 1972.

Arpaci, V.S., “Effect of Thermal Radiation on the Laminar Free Convection from a Heated Vertical Plate”, International Journal of Heat Mass Transfer, 11, 871-881, 1968.

Cess, R.D., “The Interaction of Thermal Radiation with Free Convection Heat Transfer”, International Journal of Heat Mass Transfer, 9, 1269-1277, 1966.

Chamkha, A.J., Takhar, H.S. and Soundalgekar, V.M., “Radiation Effects on Free Convection Flow Past a Semi-Infinite Vertical Plate With Mass Transfer”, Chemical Engineering Journal, 84, 335-342, 2001.

Chaudhary, R.C. and Jain, P., “An Exact Solution to the Unsteady Free-Convection Boundary-Layer Flow Past an Impulsively Started Vertical Surface with Newtonian Heating”, Journal of Engineering Physics and Thermophysics, 80, 954-960, 2007.

Das, U.N., Deka, R. and Soundalgekar, V.M., “Effects of Mass Transfer on the Flow Past an Impulsively Started Infinite Vertical Plate with Constant Heat Flux and Chemical Reaction”, Forschung im Ingenieurwesen – Engineering Research, 60, 284-287, 1994.

Das, U.N., Deka, R.K. and Soundalgekar, V.M., “Radiation Effects on Flow Past an Impulsively Started Vertical Plate – An Exact Solution”, Journal of Theoretical and Applied Fluid Mechanics, 1, 111-115, 1996.

Das, U.N., Ray, S.N. and Soundalgekar, V.M., “Mass Transfer Effects on Flow Past an Impulsively Started Infinite Vertical Plate with Constant Mass Flux – An Exact Solution”, Heat and Mass Transfer, 31, 163-167, 1996.

Gebhart, B. and Pera, L., “The Nature of Vertical Natural Convection Flows Resulting from the Combined Buoyancy Effects of Thermal and Mass Diffusion”, International Journal of Heat Mass Transfer, 14, 2025-2050, 1971.

Hossain, M.A., Alim, M.A. and Rees, D.A.S., “The Effect of Radiation on Free Convection from a Porous Vertical Plate”, International Journal of Heat and Mass Transfer, 42, 181-191, 1999.

Kaya, A., Aydin, O. and Dincer, I., “Numerical Modeling of Heat and Mass Transfer During Forced Convection Drying of Rectangular Moist Objects”, International Journal of Heat and Mass Transfer, 49, 3094-3103, 2006.

Lesnic, D., Ingham, D.B. and Pop, I., “Free Convection Boundary-Layer Flow along a Vertical Surface in a Porous Medium with Newtonian Heating”, International Journal of Heat and Mass Transfer, 42, 2621-2627, 1999.

Lesnic, D., Ingham, D.B. and Pop, I., “Free Convection from a Horizontal Surface in a Porous Medium with Newtonian Heating”, Journal of Porous Media, 3, 227-235, 2000.

Lesnic, D., Ingham, D.B., Pop, I. and Storr, C., “Free Convection Boundary-Layer Flow above a Nearly Horizontal Surface in a Porous Medium With Newtonian Heating”, Heat and Mass Transfer, 40, 665-672, 2004.

Loganathan, P. and Ganesan, P., “Effects of Radiation on Flow Past an Impulsively Started Infinite Vertical Plate with Mass Transfer”, Journal of Engineering Physics and Thermophysics, 79, 65-72, 2006.

Mebine, P. and Adigio, E.M., “Unsteady Free Convection Flow with Thermal Radiation Past a Vertical Porous Plate with Newtonian Heating”, Turkish Journal of Physics, 33, 109-119, 2009.

Merkin, J.H., “Natural-Convection Boundary-Layer Flow on a Vertical Surface with Newtonian Heating”, International Journal of Heat and Fluid Flow, 15, 392-398, 1994.

Muthucumaraswamy, R., Ganesan, P. and Soundalgekar, V.M., “Theoretical Solutions of Flow Past an Impulsively Started Vertical Plate With Variable Temperature and Mass Diffusion”, Forschung im Ingenieurwesen – Engineering Research, 66, 147-151, 2000.

Muthucumaraswamy, R., Ganesan, P. and Soundalgekar, V.M., “Heat and Mass Transfer Effects on Flow Past an Impulsively Started Vertical Plate”, Acta Mechanica, 146, 1-8, 2001.

Narahari, M. and Dutta, B.K., "Effects of Mass Transfer and Free-Convection Currents on the Flow Near a Moving Vertical Plate with Ramped Wall Temperature", Paper No. HT2009-88045, Proceedings of the ASME 2009 Heat Transfer Summer Conference, San Francisco, USA, 2009.

Narahari, M. and Ishak, A., "Radiation Effects on Free Convection Flow Near a Moving Vertical Plate with Newtonian Heating", Journal of Applied Sciences, 11, 1096-1104, 2011.

Prasad, V.R., Reddy, N.B. and Muthucumaraswamy, R., "Radiation and Mass Transfer Effects on Two-Dimensional Flow Past an Impulsively Started Infinite Vertical Plate", International Journal of Thermal Sciences, 46, 1251-1258, 2007.

Raptis, A. and Perdikis, C., "Radiation and Free Convection Flow Past a Moving Plate", International Journal of Applied Mechanical Engineering, 4, 817-821, 1999.

Salleh, M.Z., Nazar, R. and Pop, I., "Mixed Convection Boundary Layer Flow Over a Horizontal Circular Cylinder with Newtonian Heating", Heat Mass Transfer, 46, 1411-1418, 2010.

Salleh, M.Z., Nazar, R. and Pop, I., "Boundary Layer Flow and Heat Transfer Over a Stretching Sheet with Newtonian Heating", Journal of the Taiwan Institute of Chemical Engineers, 41, 651-655, 2010.

Salleh, M.Z., Nazar, R., Arifin, N.M., Pop, I. and Merkin, J.H., "Forced-Convection Heat Transfer Over a Circular Cylinder with Newtonian Heating", Journal of Engineering Mathematics, 69, 101-110, 2011.

Siegel, R. and Howell, J.R., Thermal Radiation Heat Transfer, 4th edition, Taylor & Francis, New York, 2002.

Soundalgekar, V.M., "Effects of Mass Transfer and Free Convection Currents on the Flow Past an Impulsively Started Vertical Plate", ASME Journal of Applied Mechanics, 46, 757-760, 1979.

Soundalgekar, V.M., Birajdar, N.S. and Darwhekar, V.K., "Mass-Transfer Effects on the Flow Past an Impulsively Started Infinite Vertical Plate with Variable Temperature or Constant Heat Flux", Astrophysics and Space Science, 100, 159-164, 1984.

Soundalgekar, V.M., Pohanerkar, S.G. and Lahurikar, R.M., "Effects of Mass Transfer and Heat Sources on the Flow Past an Accelerated Infinite Vertical Plate", Forschung im Ingenieurwesen – Engineering Research, 58, 63-66, 1992.